



Yu, Z. J., Chen, H., Lennox, A. J. J., Yan, L. J., Liu, X. F., Xu, D. D., ... Luo, S. P. (2019). Heteroleptic copper(I) photosensitizers with carbazole-substituted phenanthroline ligands: Synthesis, photophysical properties and application to photocatalytic H₂ generation. *Dyes and Pigments*, 162, 771-775. <https://doi.org/10.1016/j.dyepig.2018.10.067>

Peer reviewed version

License (if available):
CC BY-NC-ND

Link to published version (if available):
[10.1016/j.dyepig.2018.10.067](https://doi.org/10.1016/j.dyepig.2018.10.067)

[Link to publication record in Explore Bristol Research](#)
PDF-document

This is the author accepted manuscript (AAM). The final published version (version of record) is available online via Elsevier at <https://www.sciencedirect.com/science/article/pii/S0143720818320795>. Please refer to any applicable terms of use of the publisher.

University of Bristol - Explore Bristol Research

General rights

This document is made available in accordance with publisher policies. Please cite only the published version using the reference above. Full terms of use are available:
<http://www.bristol.ac.uk/pure/about/ebr-terms>

Heteroleptic copper(I) photosensitizers with carbazole-substituted phenanthroline ligands: synthesis, photophysical properties and application to photocatalytic H₂ generation

Zhe-Jian Yu ^a, Hao Chen ^a, Alastair J. J. Lennox ^b, Li-Juan Yan ^c, Xue-Fen Liu ^d, Dan-Dan Xu ^a, Feng Chen ^a, Liang-Xuan Xu ^a, Yang Li ^a, Qing-An Wu ^a and Shu-Ping Luo ^{a,*}

^a State Key Laboratory Breeding Base of Green Chemistry-Synthesis Technology, Zhejiang University of Technology, 310014, Hangzhou (China)

^b School of Chemistry, University of Bristol, Cantock's Close, Bristol, BS8 1TS (UK)

^c College of Electronics & Information Engineering, Guangdong Ocean University, 524088, Zhanjiang (China)

^d Qiangjiang College, Hangzhou Normal University, 310012 Hangzhou (China)

Abstract: A series of novel 4,7-dicarbazol-1,10-phenanthroline bidentate *N*-ligands have been designed and synthesized, and applied in heteroleptic copper complexes [Cu(P[^]P)(N[^]N)]⁺ as photosensitizers (PS) for light-driven water reduction. In combination with a water reduction catalyst (WRC), Fe₃CO₁₂, photocatalytic performances up to 1036 turnover numbers (TON) were reached. This excellent performance can be attributed to the introduction of carbazole groups to the phenanthroline backbone, which can increase the quantum yield, decrease the reduction potential of the copper complexes and switch the excited state quenching mechanism from reductive to oxidative. By means of DFT calculations, it has been established that the carbazole substituent contributes most significantly to the HOMO of these complexes.

Introduction

Limited fossil fuel reserves and excessive CO₂ emissions require an urgent demand for renewable and clean power sources.¹⁻² Hydrogen (H₂) gas is an environmentally clean, carbon-free and renewable fuel, and is considered an ideal candidate for an economically and socially sustainable future. Decomposition of water directly by solar energy translates solar energy into chemical energy, and is a goal at the frontier of solar energy utilization.³ Typical photocatalytic systems for proton reduction consist of three components: a photosensitizer (PS) catalyst to absorb the energy of light, a water reduction catalyst (WRC) and a sacrificial electron donor (SR). The efficient conversion of light by the photosensitizer with a stable, inexpensive and non-toxic catalyst is fundamental to the success of such a strategy, but is currently the key restriction in the efficiency of solar energy utilization. In recent years, most efforts in this area have involved the use of noble-metal-based PS and WRC.⁴ To date, the most widely used photosensitizers⁵⁻⁶ are those based on second or third row transition metals, such as Ru⁷, Re⁸, Ir⁹, and Pt¹⁰. However, these metals are of high cost and low natural abundance, generating expensive, large scale production costs.¹¹⁻¹³ One potential and viable solution is to use cheaper and more abundant first-row transition metals. Toward this end, photosensitizers based on Cu(I) have attracted great attention, as copper is a metal of low toxicity and has been successfully tested in typical photocatalytic systems.¹⁴⁻¹⁵

The carbazole moiety has been used in organic dyes featuring thermally activated delayed fluorescence (TADF) in recent years,¹⁶⁻¹⁷ because of the electron-rich, rigid, nitrogen-containing fused rings. In addition, carbazole contains a large π-conjugated structure and possesses an excellent ability for electron transfer within a molecule.¹⁸⁻¹⁹ In our previous works, we have reported a series of Cu(I) compounds decorated with no heterocyclic ring substituents.²⁰ Due to the high photoluminescence and electroluminescence efficiencies of carbazole, we were interested to investigate the efficiency of carbazole-substituted dyes as photosensitizers for water reduction.

In this report, we apply a class of carbazole-substituted phenanthrolines as bidentate *N*-ligands to copper and use these photosensitizers for solar energy driven water splitting. Their photophysical properties and electroluminescence behaviors are studied in detail and compared experimentally and theoretically.

Results and discussion

Synthesis and structure

The synthesis of three carbazole-containing ligands (L1, L2 and L3) was achieved according to [Scheme 1](#). The 4,7-dichloro-1,10-phenanthroline was synthesized according to a procedure described in the literature.²¹ A nucleophilic aromatic substitution reaction was used to couple the phenanthroline precursor with the carbazole, followed by a nucleophilic addition of lithium alkylide.²²⁻²³ All the metal complexes were prepared by an in-situ synthetic method, reacting $\text{Cu}(\text{CH}_3\text{CN})_4\text{PF}_6$, Xantphos with the appropriate *N*-ligand (CuPS1, CuPS2 or CuPS3; [Scheme 1](#)).

Scheme 1.

Photophysical properties

UV/vis absorption and photoluminescence (PL) spectra of CuPS1, CuPS2, CuPS3 in THF are shown in [Figure 1](#) and summarized in [Table 1](#). All complexes displayed a strong absorption in the visible region with a typical absorption band around 390 nm. The low-energy absorption bands from 390 nm extending to the visible region are mainly dominated by intraligand charge transfer (ILCT) transitions as reported for other Cu(I) compounds.²⁴ Due to the deactivation of the ILCT excited states, all of these compounds show strong room-temperature photoluminescence. The emission spectra of the photosensitizers are also shown in [Fig. 1](#). All of these complexes peak at around 545 nm. Compared to other complexes of the type $[\text{Cu}(\text{N}^{\wedge}\text{N})(\text{P}^{\wedge}\text{P})]^+$ with other *N*-ligands, such as bathocuproine (BCP), these complexes show the highest molar absorption coefficient (ϵ) and quantum yields (F_{abs}), but lower lifetimes (τ) due to the introduction of two fluorescence donors (carbazole and Xantphos). Moreover, compared to photosensitizer CuPS1 ($\text{R}_2 = \text{Me}$), CuPS2 and CuPS3 ($\text{R}_2 = i\text{-Pr}$) exhibit a further blue-shift in a THF solution, confirming the effectiveness with which the Jahn–Teller (flattening) distortion of the initially populated Franck-Condon excited state is hindered.²⁵ Thus, this clearly demonstrates the existence of higher fluorescence quantum yields and longer excitation lifetimes, which may improve the activity of copper complexes for water reduction.

Figure 1.

Table 1.

In order to evaluate the differences in the chemical and physical properties of a variety of copper complexes with these novel bidentate *N*-ligands, Density Functional Theory (DFT) and Time-Dependent DFT (TD-DFT) calculations (see [Figure 2](#) and [Table S2-S4](#)) were undertaken (simplified P-ligands replaced Xantphos to reduce complexity). This system based on the optimized geometries at the B3LYP/LANL2DZ and

the polarizable continuum model (PCM) levels of theory. For all of these photosensitizers, the electron density of the HOMO was found to be mainly distributed over the carbazole moiety, whereas the LUMO has main contributions from the phenanthroline moiety.

Figure 2.

Electrochemical studies

To further understand the properties of complexes CuPS1, CuPS2, and CuPS3, cyclic and differential pulse voltammetry were undertaken in acetonitrile (Figure 3 and Table S1). Each of these complexes exhibit reversible single-electron couples. Their reduction potential values and electrochemical behavior are both similar to previously reported studies of related $[\text{Cu}(\text{N}^{\wedge}\text{N})_2]^+$ complexes.²⁵ The reversible redox wave at -0.93 V should be associated with a reduction of the phenanthroline ligand, which appears at a more negative potential than the reduction peak of the WRC. As compared to complexes with bathocuproine ligands, *i.e.*, without the carbazole moiety, this reversible redox couple is about 1 V less negative.²⁵

Figure 3.

Photocatalytic hydrogen production

We initiated our investigation into the water splitting reduction reaction by establishing the volume of gas generated in the absence of catalyst (Table S5), which was found to be negligible. According to the conditions in our recent communication,²⁶ the photocatalytic reactions were performed with heteroleptic $[\text{Cu}(\text{N}^{\wedge}\text{N})(\text{P}^{\wedge}\text{P})]\text{PF}_6$ complexes as photosensitizers, a water-reduction catalyst (WRC) and triethylamine as a sacrificial reductant (SR). A mixture of THF, triethylamine TEA and water (THF/TEA/H₂O = 4:3:1) was used as a reaction solution.^{25, 27-30} These conditions ensured an excess of sacrificial electron donor and water were present at any time during the reaction. All experiments were repeated at least twice.

The water-reduction catalyst dependence of the water reduction activity was first evaluated with photosensitizer CuPS2, Table 2. Both K_2PtCl_4 and $\text{Co}(\text{bpy})_3\text{Cl}_2$ displayed poor activities (Table 2, entry 2 and 4), while the highest performances were obtained with $\text{Fe}_3(\text{CO})_{12}$ (Table 2, entry 1), which gave a turnover number (TON) of 546 after 15.0 h, compared with a TON of 462 for PdCl_2 (Table 2, entry 3). Due to the greatest ability to generate hydrogen from water, $\text{Fe}_3(\text{CO})_{12}$ was finally selected as a suitable water-reduction catalyst to compare the novel photosensitizers. The concentration of WRC was next varied. Interestingly, with a reduction of $\text{Fe}_3(\text{CO})_{12}$ from 2 mM to 0.25 mM, the TON of CuPS increased from 42 to 1036 (Figure 4). Similar to our previous work,³¹ a higher WRC / PS ratio promotes reaction between $\text{Fe}_3(\text{CO})_{12}$ and Xantphos, in which the concentration of active $[\text{Cu}(\text{N}^{\wedge}\text{N})(\text{P}^{\wedge}\text{P})]^+$ is decreased. However, when 0.1 mM $\text{Fe}_3(\text{CO})_{12}$ was added, the TON decreased to 523, which may be due to the low concentration of catalyst, thus leading to a decrease in the stability of the photocatalytic system. In the end, 0.25 mM was selected as the best concentration of $\text{Fe}_3(\text{CO})_{12}$. Under these conditions, the rate of hydrogen evolution ceased after 24 h, but the addition of more PS reestablished water reduction (Figure S19), clearly demonstrating that the decay of PS leads to a decline of gas evolution. To establish what fraction of incident photons leads to gas evolution, the incident photon to hydrogen efficiency (IPE) was measured (Figure S20 and Table S6), and determined as a maximum of 2.95% at 450 nm and 400 nm.

Table 2.

Figure 4.

We performed Stern-Volmer quenching studies in order to establish the quenching mode of the excited state of the PS (Figure S21). The initial step of the photocatalytic cycle could either be a reductive quenching of the excited state of CuPS quenched by an electron transfer from TEA, or an oxidative quenching by the catalyst $\text{Fe}_3(\text{CO})_{12}$. We found in fact that the PS was quenched by $\text{Fe}_3(\text{CO})_{12}$ with a rate constant (k_q) of $1.34 \times 10^{10} \text{ M}^{-1} \text{ s}^{-1}$ (Figure 5a). With an increasing concentration of TEA, the luminescence ratio of CuPS2 was totally unaffected (Figure 5b). This remarkable finding is in direct contrast to that observed in our previous work without carbazole-containing ligands,^{20, 32} where TEA, rather than $\text{Fe}_3(\text{CO})_{12}$, quenched the excited state. Thus, the carbazole moieties are inducing a switch in the mechanism from reductive to oxidative quenching.

Figure 5.

Cu complexes bearing Xantphos and these novel N-ligands have resulted in significant hydrogen production (Table 3, entries 1-3). The highest activity was obtained when N ligand L2 was used and 44.4 mL of hydrogen was produced during 24 hours, which correlates to a TON for CuPS2 of up to 1036 (Table 3, entry 2). So far, CuPSs containing carbazole groups at the 4,7-positions have been found to be active in the photocatalytic proton reduction. In the ground state, the heteroleptic copper complex (CuPS) exhibits a distorted tetrahedral structure, but after photoexcitation, the structure is transferred to a triplet excited state.³³⁻³⁵ Due to the HOMO being located on the carbazole moiety, it is helpful to prevent the transition to square planar geometry. It can be noted that this configuration is likely to promote a more stable photocatalytic H_2 production system, suggesting superior performances as a PS.

Table 3.

Conclusions

In summary, we have shown that heteroleptic Cu-based photosensitizer (PS) containing dicarbazole-phenanthroline ligands can be applied to photocatalytic proton reduction using $\text{Fe}_3\text{CO}_{12}$ as a water reduction catalyst. The *in situ* generated cationic Cu complexes display turnover numbers (TON) up to 1036, showing highly effective sensitizers for visible-light-driven hydrogen generation. The absorption spectra, luminescence properties and redox behavior of the metal complexes have been studied and exhibit the typical MLCT emissions of Cu(I) complexes. Notably, thanks to long lifetimes of the excited states, high stability towards atmospheric conditions and a switch in quenching mechanism, these novel complexes display an excellent ability to generate hydrogen from water. The results of this study will be important for the design and development of new efficient cuprous complexes that can be used in photosensitizers for water splitting.

Acknowledgements

Financial support by the National Natural Science Foundation of China (No. 21376222), the Natural Science Foundation of Zhejiang Province (No. LY18B060011) and the Royal Society (URF to AJJL) is gratefully acknowledged.

Keywords: Photosensitizers • Water reduction • Hydrogen production

References:

1. Xiaoning, W.; Fulei, W.; Yuanhua, S.; Hong, L., Full-Spectrum Solar-Light-Activated Photocatalysts for Light–Chemical Energy Conversion. *Adv. Energy Mater.* **2017**, *7* (23), 1700473.
2. Kim, D.; Sakimoto, K. K.; Hong, D.; Yang, P., Artificial Photosynthesis for Sustainable Fuel and Chemical Production. *Angew. Chem. Int. Ed.* **2015**, *54* (11), 3259–3266.
3. Chia, X.; Sutrisnoh, N. A. A.; Pumera, M., Tunable Pt–MoS_x Hybrid Catalysts for Hydrogen Evolution. *ACS Appl. Mat. Interfaces* **2018**, *10* (10), 8702–8711.
4. Huan, L.; Chengcheng, Z.; Xin, Z.; Han, S.; Haotian, B.; Yunxia, W.; Fengting, L.; Libing, L.; Yuguo, M.; Shu, W., Polythiophene–Peptide Biohybrid Assemblies for Enhancing Photoinduced Hydrogen Evolution. *Adv. Electron. Mater.* **2017**, *3* (11), 1700161.
5. Gueret, R.; Poulard, L.; Oshinowo, M.; Chauvin, J.; Dahmane, M.; Dupeyre, G.; Lainé, P. P.; Fortage, J.; Collomb, M.-N., Challenging the [Ru(bpy)₃]²⁺ Photosensitizer with a Triazatriangulenium Robust Organic Dye for Visible-Light-Driven Hydrogen Production in Water. *ACS Catal.* **2018**, *8* (5), 3792–3802.
6. Xinyan, G.; Yiming, L.; Qi, C.; Dahui, Z.; Yuguo, M., New Bichromophoric Triplet Photosensitizer Designs and Their Application in Triplet–Triplet Annihilation Upconversion. *Adv. Opt. Mater.* **2018**, *6* (4), 1700981.
7. Abbotto, A.; Manfredi, N., Electron-rich heteroaromatic conjugated polypyridine ruthenium sensitizers for dye-sensitized solar cells. *Dalton Trans.* **2011**, *40* (46), 12421–12438.
8. Joshi, U.; Malkhandi, S.; Ren, Y.; Tan, T. L.; Chiam, S. Y.; Yeo, B. S., Ruthenium–Tungsten Composite Catalyst for the Efficient and Contamination-Resistant Electrochemical Evolution of Hydrogen. *ACS Appl. Mat. Interfaces* **2018**, *10* (7), 6354–6360.
9. Singhanian, A.; Bhaskarwar, A. N., Effect of rare earth (RE – La, Pr, Nd) metal-doped ceria nanoparticles on catalytic hydrogen iodide decomposition for hydrogen production. *Int J Hydrogen Energy* **2018**, *43* (10), 4818–4825.
10. Stefanie, S.; Magdalena, H.; Montaha, A.; Timo, J.; Sven, R.; Carsten, S., Experimental and Theoretical Investigation of the Light-Driven Hydrogen Evolution by Polyoxometalate–Photosensitizer Dyads. *Chem. Eur. J.* **2017**, *23* (61), 15370–15376.
11. He, Z.-D.; Wei, J.; Chen, Y.-X.; Santos, E.; Schmickler, W., Hydrogen evolution at Pt(111) – activation energy, frequency factor and hydrogen repulsion. *Electrochim. Acta* **2017**, *255*, 391–395.
12. Rao, H.; Yu, W.-Q.; Zheng, H.-Q.; Bonin, J.; Fan, Y.-T.; Hou, H.-W., Highly efficient photocatalytic hydrogen evolution from nickel quinolinethiolate complexes under visible light irradiation. *J. Power Sources* **2016**, *324*, 253–260.
13. Kankanamalage, P. H. A.; Mazumder, S.; Tiwari, V.; Kpogo, K. K.; Bernhard Schlegel, H.; Verani, C. N., Efficient electro/photocatalytic water reduction using a [NiII(N₂Py₃)₂]⁺ complex. *Chem. Commun.* **2016**, *52* (91), 13357–13360.
14. Qi, Y.-Y.; Gan, Q.; Liu, Y.-X.; Xiong, Y.-H.; Mao, Z.-W.; Le, X.-Y., Two new Cu(II) dipeptide complexes based on 5-methyl-2-(2'-pyridyl)benzimidazole as potential antimicrobial and anticancer drugs: Special exploration of their possible anticancer mechanism. *Eur. J. Med. Chem.* **2018**, *154*, 220–232.
15. Mandegarzar, S.; Raoof, J. B.; Hosseini, S. R.; Ojani, R., MOF-derived Cu-Pd/nanoporous carbon composite as an efficient catalyst for hydrogen evolution reaction: A comparison between hydrothermal and electrochemical synthesis. *Appl. Surf. Sci.* **2018**, *436*, 451–459.
16. Ni, F.; Wu, Z.; Zhu, Z.; Chen, T.; Wu, K.; Zhong, C.; An, K.; Wei, D.; Ma, D.; Yang, C., Teaching an old acceptor new tricks: rationally employing 2,1,3-benzothiadiazole as input to design a highly efficient red thermally activated delayed fluorescence emitter. *J. Mater. Chem. C* **2017**, *5* (6), 1363–1368.
17. Cho, Y. J.; Jeon, S. K.; Chin, B. D.; Yu, E.; Lee, J. Y., The Design of Dual Emitting Cores for Green Thermally Activated Delayed Fluorescent Materials. *Angew. Chem. Int. Ed.* **2015**, *54* (17), 5201–5204.
18. Xie, Y.; Li, Z., Thermally Activated Delayed Fluorescent Polymers. *J. Polym. Sci. Pol. Chem.* **2017**, *55* (4), 575–584.
19. Yang, Z.; Mao, Z.; Xie, Z.; Zhang, Y.; Liu, S.; Zhao, J.; Xu, J.; Chi, Z.; Aldred, M. P., Recent advances in organic thermally activated delayed fluorescence materials. *Chem. Soc. Rev.* **2017**, *46* (3), 915–1016.
20. Luo, S.-P.; Chen, N.-Y.; Sun, Y.-Y.; Xia, L.-M.; Wu, Z.-C.; Junge, H.; Beller, M.; Wu, Q.-A., Heteroleptic copper(I) photosensitizers of dibenzo[b,j]-1,10-phenanthroline derivatives driven hydrogen generation from water reduction. *Dyes Pigments* **2016**, *134*, 580–585.
21. Graf, G. I.; Hastreiter, D.; da Silva, L. E.; Rebelo, R. A.; Montalban, A. G.; McKillop, A., The synthesis of aromatic diazatriacycles from phenylenediamine-bis(methylene Meldrum's acid) derivatives. *Tetrahedron* **2002**, *58* (44), 9095–9100.
22. Neugebauer, F. A.; Fischer, H., tert.-Butyl-substituierte Carbazole. *Chem. Ber.* **1972**, *105* (8), 2686–2693.
23. McClenaghan, N. D.; Passalacqua, R.; Loiseau, F.; Campagna, S.; Verheyde, B.; Hameurlaine, A.; Dehaen, W., Ruthenium(II) Dendrimers Containing Carbazole-Based Chromophores as Branches. *J. Am. Chem. Soc.* **2003**, *125* (18), 5356–5365.
24. Armaroli, N.; Accorsi, G.; Holler, M.; Moudam, O.; Nierengarten, J. F.; Zhou, Z.; Wegh, R. T.; Welter, R., Highly Luminescent CuI Complexes for Light-Emitting Electrochemical Cells. *Adv. Mater.* **2006**, *18* (10), 1313–1316.
25. Mejía, E.; Luo, S.-P.; Karnahl, M.; Friedrich, A.; Tschierlei, S.; Surkus, A.-E.; Junge, H.; Gladiali, S.; Lochbrunner, S.; Beller, M., A Noble-Metal-Free System for Photocatalytic Hydrogen Production from Water. *Chem. Eur. J.* **2013**, *19* (47), 15972–15978.
26. Chen, N. Y.; Xia, L. M.; Lennox, A. J. J.; Sun, Y. Y.; Chen, H.; Jin, H. M.; Junge, H.; Wu, Q. A.; Jia, J. H.; Beller, M.; Luo, S. P., Structure-Activated Copper Photosensitizers for Photocatalytic Water Reduction. *Chem. Eur. J.* **2017**, *23* (15), 3631–3636.
27. Karnahl, M.; Mejía, E.; Rockstroh, N.; Tschierlei, S.; Luo, S.-P.; Grabow, K.; Kruth, A.; Brüser, V.; Junge, H.; Lochbrunner, S.; Beller, M., Photocatalytic Hydrogen Production with Copper Photosensitizer–Titanium Dioxide Composites. *ChemCatChem* **2014**, *6* (1), 82–86.
28. Junge, H.; Codolà, Z.; Kammer, A.; Rockstroh, N.; Karnahl, M.; Luo, S.-P.; Pohl, M.-M.; Radnik, J.; Gatla, S.; Wohlrab, S.; Lloret, J.; Costas, M.; Beller, M., Copper-based water reduction catalysts for efficient light-driven hydrogen generation. *J. Mol. Catal. A -Chem.* **2014**, *395* (Supplement C), 449–456.
29. Hollmann, D.; Karnahl, M.; Tschierlei, S.; Kailasam, K.; Schneider, M.; Radnik, J.; Grabow, K.; Bentrup, U.; Junge, H.; Beller, M.; Lochbrunner, S.; Thomas, A.; Brückner, A., Structure–Activity Relationships in Bulk Polymeric and Sol–Gel-Derived Carbon Nitrides during Photocatalytic Hydrogen Production. *Chem. Mater.* **2014**, *26* (4), 1727–1733.
30. Bokarev, S. I.; Hollmann, D.; Pazidis, A.; Neubauer, A.; Radnik, J.; Kuhn, O.; Lochbrunner, S.; Junge, H.; Beller, M.; Brückner, A., Spin density distribution after electron transfer from triethylamine to an [Ir(ppy)₂(bpy)]⁺ photosensitizer during photocatalytic water reduction. *Phys. Chem. Chem. Phys.* **2014**, *16* (10), 4789–4796.
31. Lennox, A. J. J.; Fischer, S.; Jurrat, M.; Luo, S.-P.; Rockstroh, N.; Junge, H.; Ludwig, R.; Beller, M., Copper-Based Photosensitizers in Water Reduction: A More Efficient In Situ Formed System and Improved Mechanistic Understanding. *Chem. Eur. J.* **2016**, *22* (4), 1233–1238.
32. Yuan-Yuan, S.; Hai, W.; Nan-Yu, C.; J, L. A. J.; Aleksey, F.; Liang-Min, X.; Stefan, L.; Henrik, J.; Matthias, B.; Shaolin, Z.; Shu-Ping, L., Efficient Photocatalytic Water Reduction Using In Situ Generated Knölker's Iron Complexes. *ChemCatChem* **2016**, *8* (14), 2340–2344.
33. Fischer, S.; Hollmann, D.; Tschierlei, S.; Karnahl, M.; Rockstroh, N.; Barsch, E.; Schwarzbach, P.; Luo, S.-P.; Junge, H.; Beller, M.; Lochbrunner, S.; Ludwig, R.; Brückner, A., Death and Rebirth: Photocatalytic Hydrogen Production by a Self-Organizing Copper–Iron System. *ACS Catal.* **2014**, *4* (6), 1845–1849.

-
34. Martin, H.; Stefanie, T.; Nils, R.; Mark, R.; Wolfgang, F.; Henrik, J.; Matthias, B.; Stefan, L.; Michael, K., Heteroleptic Copper Photosensitizers: Why an Extended π -System Does Not Automatically Lead to Enhanced Hydrogen Production. *Chem. Eur. J.* **2017**, *23* (2), 312-319.
35. Jaekwan, K.; Ryeol, W. D.; Young, P. S., Designing Highly Efficient CuI Photosensitizers for Photocatalytic H₂ Evolution from Water. *ChemSusChem* **2017**, *10* (9), 1883-1886.

Scheme Caption.

Scheme 1. CuPS1-3 and the synthesis of N ligands.

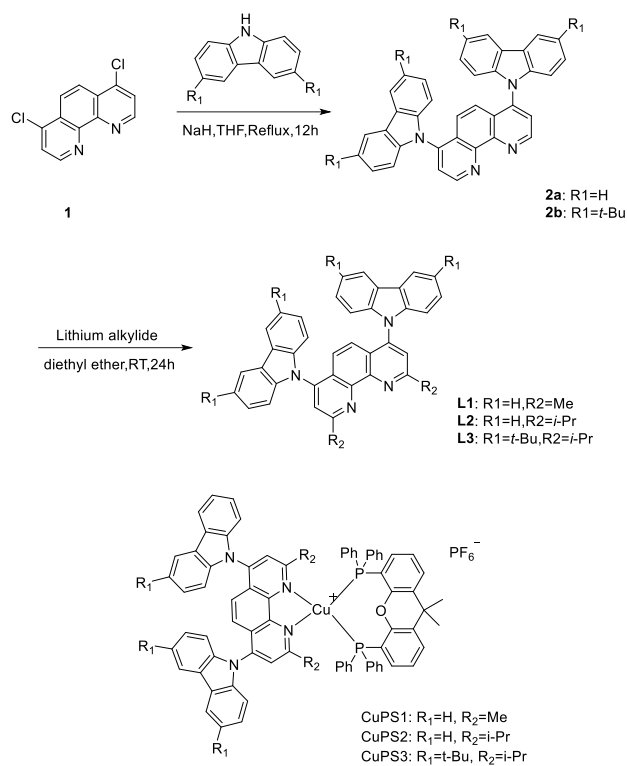


Figure Caption.

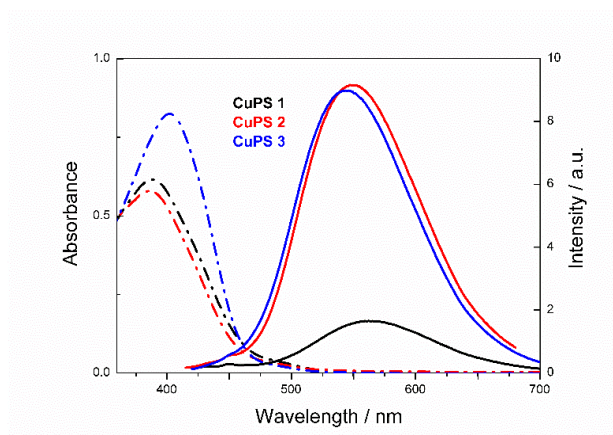


Figure 1. Absorption (dotted line) and emission (solid line) spectra for different copper(I) photosensitizers. Measurements were recorded in THF room temperature.

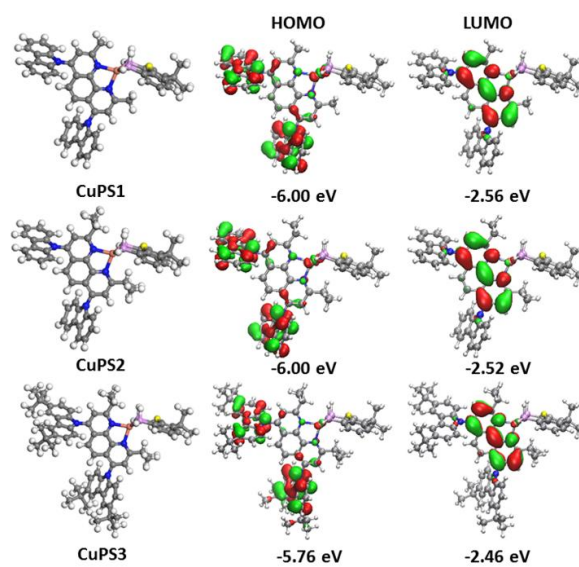


Figure 2. Representation of the optimized molecular geometry of complexes (left) and the localization of HOMO (center) and LUMO (right) orbitals.

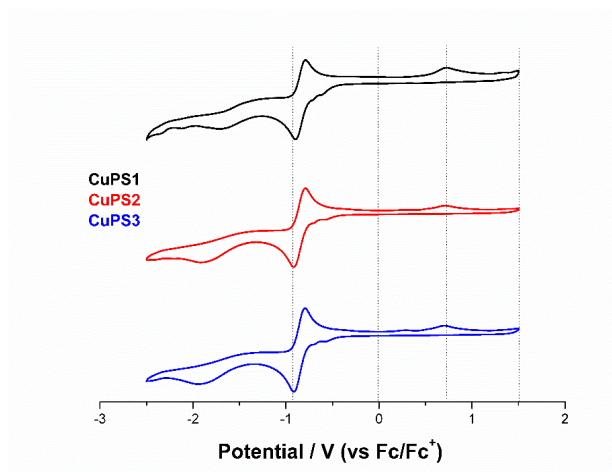


Figure 3. Cyclic and differential pulse voltammograms for different copper(I) photosensitizers.

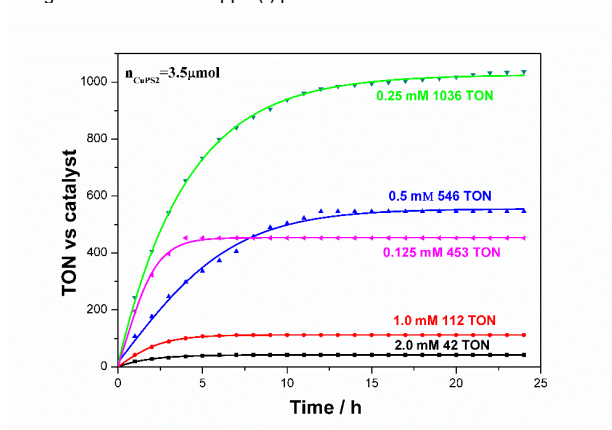


Figure 4. Photocatalytic hydrogen production (TON) as a function of time from a reaction solution (10 mL) under Xe-light irradiation in the presence of PS (3.5 μmol) and with various concentrations of Fe₃(CO)₁₂.

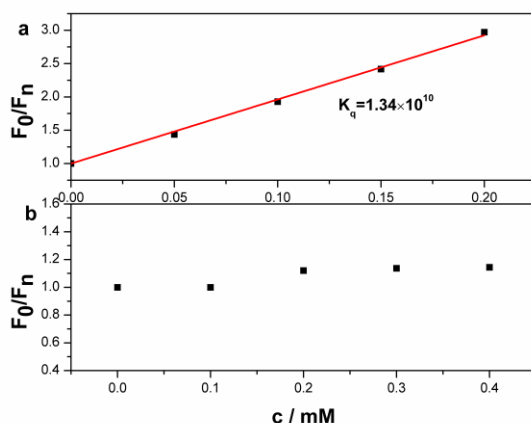


Figure 5. Stern-Volmer plots. The concentration of CuPS2 in THF was 3.5 μmol ; quenching reagents: $\text{Fe}_3\text{CO}_{12}$ (a); TEA (b).

Table 1. Electronic absorption and luminescence data for different $[\text{Cu}(\text{N}^{\wedge}\text{N})(\text{P}^{\wedge}\text{P})]\text{PF}_6$ complexes in degassed THF at room temperature.

Entry	complex	Absorption		Emission		$\tau(\text{ns})$
		λ_{max} (nm)	ϵ ($\text{M}^{-1}\text{cm}^{-1}$)	λ_{max} (nm)	$\Phi_{\text{abs}}^{[\text{a}]}$	
1	CuPS1	388	8791.7	565	0.12	322.94
2	CuPS2	386	8273.3	547	0.56	687.12
3	CuPS3	402	11783.1	544	0.48	614.12

[a] The quantum yield was measured at an optical density of about 0.1 (error: about 10%).

Table2. Results for the photocatalytic hydrogen evolution using CuPS2 in the presence of TEA as SR. Screening of WRC.^[a]

Entry ^[a]	WRC	Time(h)	Vol.H ₂ (mL)	TON _H ^[b]
1	$\text{Fe}_3(\text{CO})_{12}$	15	23.4	546
2	K_2PtCl_4	10	7.2	168
3	PdCl_2	8	16.8	392
4	$\text{Co}(\text{bpy})_3\text{Cl}_2$	3	5	116
5	$\text{PdCl}_2 + \text{PPh}_3^{[\text{c}]}$	4	3.8	89

[a] Reaction conditions: CuPS (3.5 μmol), catalyst (5 μmol), 10mL THF/TEA/H₂O(4:3:1), 25°C, Xe-light irradiation (output 5 W), without light filter, gas evolution quantitatively measured via automatic gas burettes, gas analysis via GC. All given values are the averages of at least two experiments. [b] $\text{TON}_H = n_H/n_{\text{Cu}}$. [c] WRC (5 μmol , $\text{PdCl}_2/\text{PPh}_3=1:1$)

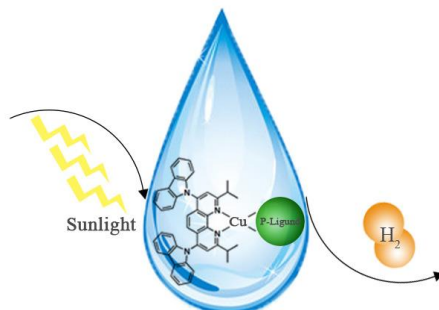
Table 3. Results for the photocatalytic water reduction using Cu(I) PS in the presence of $\text{Fe}_3(\text{CO})_{12}$ as WRC and TEA as SR.^[a]

Entry	Complexes	Time (h)	Vol.H ₂ (mL)	TON _H ^[b]
1	CuPS1	24	17.1	399
2	CuPS2	24	44.4	1036
3	CuPS3	24	42.2	984

[a] Reaction conditions: CuPS (3.5 μmol), $[\text{Fe}_3(\text{CO})_{12}]$ (2.5 μmol), 10mL THF/TEA/ H_2O (4:3:1), 25°C, Xe-light irradiation (output 5 W), without light filter, gas evolution quantitatively measured via automatic gas burettes, gas analysis via GC. All given values are the averages of at least two experiments. The results of each same experiment differ between 1 and 17%. [b] $\text{TON}_\text{H} = n_\text{H}/n_\text{Cu}$.

COMMUNICATION

A series of novel 4,7-dicarbazol-1,10-phenanthroline bidentate *N*-ligands have been designed and synthesized. Applied in water splitting system, the excellent performance up to 1036 turnover numbers can be contribute to the introduction of carbazole groups by DFT calculation. The excited state quenching mechanism is switched from reductive to oxidative due to this unique structure-property correlation.



Zhe-Jian Yu ^a, Hao Chen ^a,
Alastair J. J. Lennox ^b, li-Juan
Yan ^c, Xue-Fen Liu ^d, Dan-Dan
Xu ^a, Feng Chen ^a, Liang-Xuan
Xu ^a, Yang Li ^a, Qing-An Wu ^a
and Shu-Ping Luo ^{a,*}

Page No. – Page No.

**Heteroleptic copper(I)
photosensitizers with
carbazole-substituted
phenanthroline ligands:
synthesis, photophysical
properties and application to
photocatalytic H₂ generation**